



HAL
open science

Transcriptional landscape of the interaction of human Mesenchymal Stem Cells with Glioblastoma in bioprinted co-cultures

Lisa Oliver, Yuna Landais, Catherine Gratas, Pierre-François Cartron, François Paris, Dominique Heymann, François Vallette, Aurelien Serandour

► **To cite this version:**

Lisa Oliver, Yuna Landais, Catherine Gratas, Pierre-François Cartron, François Paris, et al.. Transcriptional landscape of the interaction of human Mesenchymal Stem Cells with Glioblastoma in bioprinted co-cultures. *Stem Cell Research and Therapy*, 2024, 15 (1), pp.424. 10.1186/s13287-024-04022-6 . inserm-04878879

HAL Id: inserm-04878879

<https://inserm.hal.science/inserm-04878879v1>

Submitted on 10 Jan 2025

HAL is a multi-disciplinary open access archive for the deposit and dissemination of scientific research documents, whether they are published or not. The documents may come from teaching and research institutions in France or abroad, or from public or private research centers.

L'archive ouverte pluridisciplinaire **HAL**, est destinée au dépôt et à la diffusion de documents scientifiques de niveau recherche, publiés ou non, émanant des établissements d'enseignement et de recherche français ou étrangers, des laboratoires publics ou privés.




Distributed under a Creative Commons Attribution 4.0 International License

RESEARCH

Open Access



Transcriptional landscape of the interaction of human Mesenchymal Stem Cells with Glioblastoma in bioprinted co-cultures

Lisa Oliver^{1,2}, Yuna Landais^{1,6}, Catherine Gratas^{1,2}, Pierre-François Cartron^{1,3}, François Paris^{1,3}, Dominique Heymann^{3,4}, François M. Vallette^{1,3*}  and Aurelien Serandour^{5*}

Abstract

Background The interaction between mesenchymal stem cells (MSC) and Glioblastoma (GBM), although potentially of the highest importance, is ill-understood. This is due, in part, to the lack of relevant experimental models. The similarity between the in vitro situations and the in vivo situation can be improved by 3D co-culture as it reproduces key cell–cell interactions between the tumor microenvironment (TME) and cancer cells.

Methods MSC Can acquired characteristics of cancer associated fibroblasts (CAF) by being cultured with conditioned medium from GBM cultures and thus are called MSC^{CAF}. We co Cultured MSC^{CAF} with patient derived GBM in a scaffold 3D bioprinted model. We studied the response to current GBM therapy (e.g. Temozolomide + /Radiation) on the co cultures by bulk transcriptomic (RNA Seq) and epigenetic (ATAC Seq) analyses

Results The transcriptomic modifications induced by standard GBM treatment in bioprinted scaffolds of mono- or co-cultures of GBM ± MSC can be analyzed. We found that mitochondrial encoded OXPHOS genes are overexpressed under these conditions and are modified by both co-culture and treatment (chemotherapy ± radiation). We have identified two new markers of MSC/GBM interactions, one epigenetically regulated (i.e. TREM-1) associated with an increased overall survival in GBM patients and another implicated in post-transcriptional regulation (i.e. the long non-coding RNA, miR3681HG), which is associated with a reduced overall survival in GBM patients.

Keywords Mesenchymal stromal/stem cell, Co-culture, 3D tumor model, Bioprinting, Response to treatment, Glioblastoma

Introduction

Glioblastoma (GBM) is the predominant primary cancer in human adults with a median survival following diagnosis of 12 to 15 months, with less than 10% of people surviving longer than five years [1]. The most current common treatment for GBM is a combination of complete (when possible) surgical resection, followed by radiotherapy and concomitant chemotherapy with the alkylating agent Temozolomide (TMZ) [2]. GBM are extremely heterogeneous and exhibit a very complex tumor microenvironment (TME), which render these tumors difficult to treat [3]. Today the main axis of research emphasizes on new therapies that are more

*Correspondence:

François M. Vallette

francois.vallette@univ-nantes.fr

Aurelien Serandour

aurelien.serandour@univ-nantes.fr

¹ Nantes Université, INSERM, CRCI2NA-INSERM U1307, 4407 Nantes, France

² Centre Hospitalier-Universitaire (CHU) de Nantes, 44007 Nantes, France

³ Institut de Cancérologie de L'Ouest, 44805 Saint-Herblain, France

⁴ Nantes Université, CNRS, US2B-UMR 6286, 44000 Nantes, France

⁵ Center for Research in Transplantation and Translational Immunology, Nantes Université, Ecole Centrale de Nantes, INSERM, CR2TI, UMR 1064, 4407 Nantes, France

⁶ Present Address: One Biosciences, Paris, France



© The Author(s) 2024. **Open Access** This article is licensed under a Creative Commons Attribution-NonCommercial-NoDerivatives 4.0 International License, which permits any non-commercial use, sharing, distribution and reproduction in any medium or format, as long as you give appropriate credit to the original author(s) and the source, provide a link to the Creative Commons licence, and indicate if you modified the licensed material. You do not have permission under this licence to share adapted material derived from this article or parts of it. The images or other third party material in this article are included in the article's Creative Commons licence, unless indicated otherwise in a credit line to the material. If material is not included in the article's Creative Commons licence and your intended use is not permitted by statutory regulation or exceeds the permitted use, you will need to obtain permission directly from the copyright holder. To view a copy of this licence, visit <http://creativecommons.org/licenses/by-nc-nd/4.0/>.

“patient-specific” and which take into account a prediction on the mechanisms of resistance [4]. One way to achieve this goal is to use accurate *in vitro* tests that allow drug or innovative treatment screening on a personalized basis [5]. Among the cells present in the GBM microenvironment are the mesenchymal stem cells (MSC), the origins of which are ill-defined [6, 7]. Of note, the presence of MSC has been correlated with the survival of the patients [8]. However, so far, no clear mechanisms have been established to explain both the tropism and the mechanism(s) of action of MSC in GBM [9]. We have recently shown, in three-dimensional (3D) co-cultures, that the influences of MSC on GBM are multiple and involve both molecule and organelle transfers through connecting structures such as tunneling nanotubes (TNT) [10] and extracellular vesicles (EV) [11]. Strikingly, the co-culture of MSC and GBM affect both cellular types as, for example, it allows MSC to acquire a cancer-associated fibroblast (CAF) phenotype and properties that are specific for each GBM [12].

The current paradigm of *in vitro* studies is currently shifting from the classical two-dimensional (2D) to 3D-cultures. 3D-cultures can be developed with or without a scaffold. Scaffold-based 3D-cultures can use solid scaffold or hydrogels derived from extracellular matrix, proteins, polymer and many other materials. It is expected that 3D-cultures could influence the nature and the extent of the results obtained in cancer studies and could replace animal studies. 3D-cultures appear to effectively address many of the limitations commonly encountered in 2D-cultures and to mirror more closely the patient tumors [13]. Specifically, 3D-cultures reproduce key structural mechanical constraints that in turn can modify tumor growth kinetics or resistance to treatments [14]. However, one has to keep in mind that the most relevant 3D cancer model has certainly to be selected for each type of cancer studied and for its specific purpose [14, 15]. One key feature of 3D-culture is a more accurate reproduction than 2D system of cell–cell interactions and the molecular mechanisms involved (e.g. differentiation, proliferation, vitality, gene expression, responsiveness to stimuli and drug metabolism). Numerous organoid/tumoroid models have been published so far and the introduction of scaffolds in the culture seems to provide a simpler, safer and more reliable approach for cancer research [5]. Using the scaffold technique, cells can be cultured in a variety of culturing tools including animal extracellular matrix extract that could amplify the similarity the *in vivo* conditions.

We have developed over the recent years a simple scaffold-free method for 3D co-cultures using primary GBM cells derived from patients with human MSC derived from healthy donor to mimic the interactions of TME

cells with cancer cells [10, 12]. However, this model lacked some important tumor features such as the rigidity or stiffness of the tissue of origin. The utilization of *in vitro* techniques using scaffold mimicking cancer cell interaction with non-tumor cells present in the TME and the extracellular matrix (ECM) are increasing the comprehension of molecular and cellular interactions controlling cancer progression. In particular, these models have enabled researchers to understand the influence of ECM on the invasive nature of tumors but there are less studies on the cellular interactions in GBM [16, 17]. The use of 3D bioprinting techniques offers several advantages for this project. This approach allows the recreation of realistic 3D models, faithfully reproducing tissue structures and cellular interactions. In addition, it offers precise control of experimental conditions, favoring the reproduction of physiological environments relevant for the study of interactions between GBM and CAF [13].

Here, we used a bioprinting device (INKREDIBLE™ from Cellink) to recreate GBM environment and then analyze the transcriptomes of tumoroids after the conventional Stupp treatment: a combination of chemotherapy (TMZ) and ionizing radiation (IR) [2].

Materials and Methods

Materials

Unless stated otherwise, all cell culture material was obtained from Life Technologies (Cergy Pontoise, France) and chemicals were from Sigma-Aldrich (St. Louis, MO, USA).

Methods

Cell Culture

After informed consent, tumor samples classified as GBM, based on the World Health Organization criteria, were obtained from patients undergoing surgical intervention at the Department of Neurosurgery at “Centre Hospitalier Universitaire de Nantes” and the “Tumorothèque IRCNA” as stated in Salaud et al. [10]. Within 4 h after surgical removal, patient-derived cells were recuperated after mechanical dissociation, as described earlier [10]. All procedures involving human participants were in accordance with the ethical standards of the ethic national research committee and with the 1964 Helsinki declaration and its later amendments or comparable ethical standards. Primary GBM cells were cultured in defined medium (DMEM/F12 supplemented with 2 mM L-glutamine, N2 and B27 supplement, 2 µg/mL heparin, 40 ng/mL EGF, 40 ng/mL bFGF, 100 U/mL penicillin, and 100 µg/mL streptomycin). The medium was changed by the removal of about 70% every 2–3 days. All the experiments with primary GBM cells were performed at early passages.

MSC were obtained from the “Tumorothèque IRCNA” and cultured in MEM α containing ribonucleosides and deoxyribonucleosides supplemented with 20% heat-inactivated foetal calf serum, 5 ng/mL bFGF, 100 U/mL penicillin, and 100 μ g/mL streptomycin as previously described [18]. To prepare MSC^{CAF}: MSC were cultured in conditioned medium obtained from GBM cultures and defined medium at a ratio of 30:70 for at least 7 days before use. MSC^{CAF} were characterized as described earlier [10–12]. Cells were cultured in an incubator at 37°C, 5% CO₂ and 95% humidity and tested for mycoplasma regularly.

Scaffold Formation

50 μ L cell suspension (3×10^7 GBM \pm 1.6×10^6 MSC^{CAF}) were re-suspended in 3 mL bioink and then bioprinted using the Inkredible™ (Cellink, Gothenburg, Sweden) into 12-well plates (Fig. 1A). Cellink bioink is composed of non-animal derived polysaccharide components only, including alginate and highly hydrated cellulose nanofibrils (www.cellink.com). The scaffolds were incubated in 200 μ L 100 mM Ca₂Cl for 3 min at room temperature and then incubated in 1 mL defined medium (DM) for 30 min at 37°C after which the medium was replaced by 1,5 mL

fresh medium. The culture medium was replaced every 2–3 days over the time of the experiment. Once tumoroid formation was confirmed, the scaffolds were treated with 50 μ M TMZ with or without γ -irradiation using a Faxitron CP160 irradiator (Faxitron X-ray Corporation, Villepinte, France) at a dose rate of 1.48 Gy/minute.

FACS analysis, immunocytochemistry and immunohistochemistry

Biospheres were dissociated manually; cells were recuperated and washed then incubated 30 min with the primary antibody CD133-APC, CD44-APC, CD10-BV420 or CD90-PE. Data acquisition was performed on a FACS CANTO II (Becton Dickinson) and analyzed using the FlowLogic software. Cell cycle status analyses were performed by FACS using a kit from ThermoFisher Scientific (France) according to the manufacturer’s instructions (www.thermofisher.com).

For immunocytochemistry, biospheres were fixed with 4% paraformaldehyde for 1 h then permeabilized with 0.1% Triton X-100 for 30 min saturated with 5% BSA and then incubated with rabbit anti-human nestin (Proteintech, Rosemont, IL, USA) and mouse anti-human anti-GFAP (Proteintech). Secondary antibodies coupled to

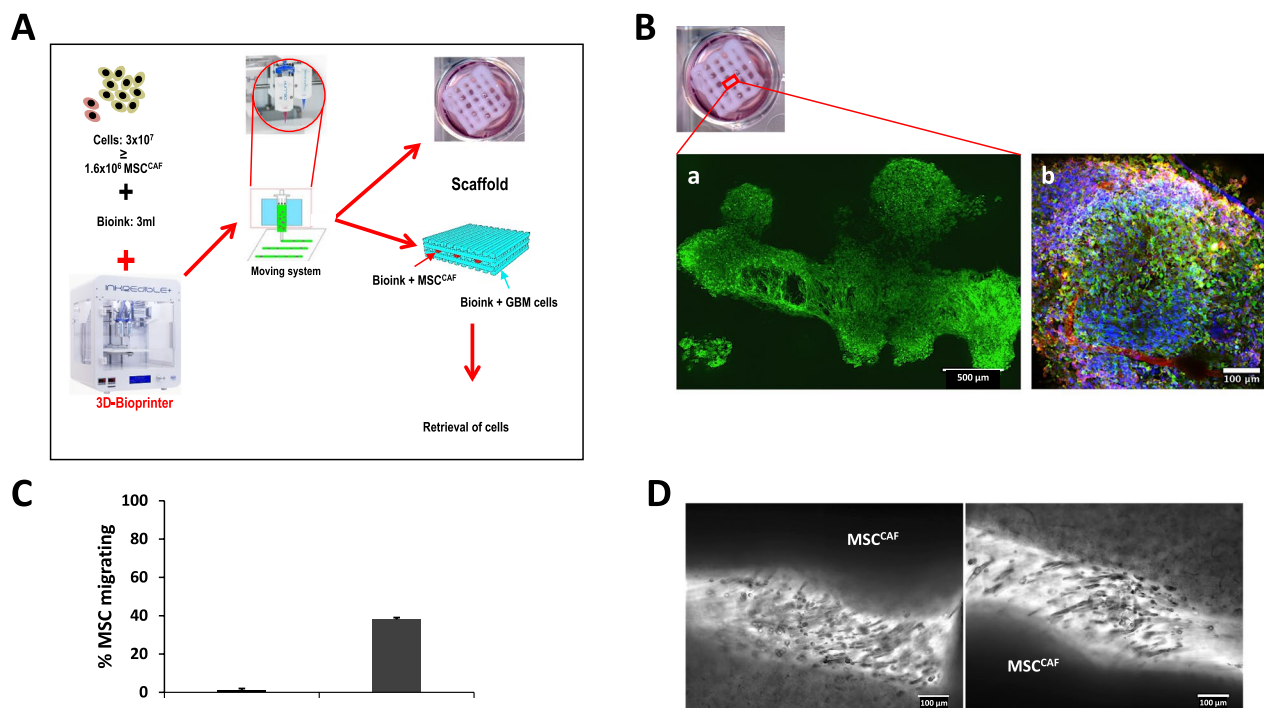


Fig. 1 Bioprinting of MSC and GBM primary cells: morphological aspects **A**) Schematic illustration of bioprinting of scaffold. **B**) Bioprinted scaffold with (a) confocal image of tumoroid structure in scaffold and (b) labeling of tumoroid with antibodies directed against GFAP (green), nestin (red) and nuclei (blue). **C**) Use of transwell to analyze the migration of MSC toward GBM in the presence of defined medium (DM) or conditioned medium (CM) obtained from 72 h GBM cultures. Images were taken 4 h later. **D**) Migration of MSC^{CAF} towards tumor cells in scaffold, beginning of tumoroid formation in scaffolds

Alexafluor-488 or -568 was added and then the sections were analyzed under a confocal microscope (Nikon A1 Rsi, MicroPicell Facility). Confocal image was acquired with confocal microscope Nikon A1 (Champigny sur Marne, France) with $\times 20$ apo objective N.A. 0.75. Image shows a maximum intensity projection of an acquisition of a mosaic 5×4 fields with 29 z-steps. Tumoroid images were obtained using a Zeiss microscope (Axio Observer and ZEN 2 program, Axio Observer, Carl Zeiss, Rueil Malmaison, France).

RNA-seq (Active Motif)

Cells were harvested, cryopreserved and sent to Active Motif® (<https://www.activemotif.com>) where RNA-seq were performed: RNA extraction, polyA⁺ RNA enrichment, directional library generation, QC of NGS library and next-generation sequencing using the Illumina platform.

Assay for Transposase-Accessible Chromatin with High-Throughput Sequencing (ATAC-seq) (Active Motif)

Cells were harvested, cryopreserved and sent to Active Motif® (<https://www.activemotif.com/>) where ATAC-seq were performed following the protocols from Buenrostro et al. 2013 [19] and Corces et al. 2017 [20]. The RNA-seq/ATAC-seq data are available in European Nucleotide Archive with the accession number PRJEB76177.

Statistics

Data were analyzed and statistical analyses were performed using GraphPad Prism 7.00 (GraphPad Software, San Diego, CA, USA).

Patients

The local ethics committee (GNEDS: Groupe Nantais d'Ethique dans le Domaine de la Santé) approved the collection and use of these data (approval on Dossier 06/15 on 8 April 2015). Written informed consent was obtained for all patients included in this study.

Results

Bioprinting of patient-derived GBM with MSC from healthy donor

Bioprinted cell co-cultures derived from GBM and MSC^{CAF} were performed as described in Materials and Methods and presented diagrammatically in Fig. 1A. Tumoroid formation was determined at the end of cultures since the complexity of tumoroid formation was not possible due to the thickness of the scaffold and the opaqueness of the matrix (Fig. 1B). Note that the heterogeneous composition of tumoroids is depicted by the presence of nestin (marker of stem cells) and GFAP

(marker of astrocytes) (Fig. 1B). Experiments were performed to validate the attraction of MSC to GBM cells; MSC were plated in transwell with a membrane pore of 8 μm then inserted into wells containing either DM or GBM-conditioned medium (CM). Four hours later the percentage MSC migrated through the membrane were determined. Data presented in Fig. 1C show that about 40% of the MSC exposed to CM traversed the membrane compared to almost none in the wells containing DM. MSC exposed to CM acquired some CAF characteristics to become MSC^{CAF} as described earlier [10–12]. Since it is difficult to observe 3D tumoroid formation in scaffolds, experiments were performed placing MSC^{CAF} and GBM cells in different areas in the scaffold and then analyzing the interaction(s) between the cells. As can be seen in Fig. 1D, in co-culture scaffolds, MSC^{CAF} migrated towards GBM cells. We did not observe the opposite, i.e. migration of GBM cells toward MSC^{CAF}.

Effect of MSC on GBM proliferation and response to treatment with TMZ and/or IR

After the apparition of tumoroid formation, GBM monoculture (Gb) and GBM + MSC^{CAF} co-culture (GbT) were treated (or not, control) with TMZ (50 $\mu\text{g}/\text{mL}$), radiation (2 Gy) or both. The effects of MSC^{CAF} on the GBM response to treatment indicated a differential sensitivity toward both TMZ and/or IR (Fig. 2A). As previously reported [10, 12], co-culture with MSC induced a better protection to the treatments for GbT compared to Gb. Of note, analyses of MSC markers (CD90, CD10) indicated that MSC^{CAF} were no longer present in the scaffolds at the time of the analysis (Fig. 2B) as previously described in another 3D model [12].

Next, we analyzed cell proliferation using the diameters distribution of spheroids as described before [10, 12]. As shown in Fig. 2C, GbT spheroids exhibited larger diameters, reflecting an increase in cell numbers. Cell cycle status analyses indicated only minor differences between Gb and GbT but a more differential response toward treatments, which affected cell cycle more in Gb than in GbT (Fig. 2D, E).

Effect of co-culture and treatments on the GBM transcriptomic landscapes

Only cancer cells transcriptomes were expected to be present in the samples used for RNA-seq as MSC^{CAF} antigens were not found in control and treated Gb or GbT (Fig. 2B). This implied that transcriptomics analyses will reveal only cancer cells alterations. For transcriptomic analyses of tumoroids, cells were retrieved from the scaffolds by incubation with 100 mM Na-citrate.

From the analyses of count data from RNA-seq, we used DESeq2 R package to determine differentially

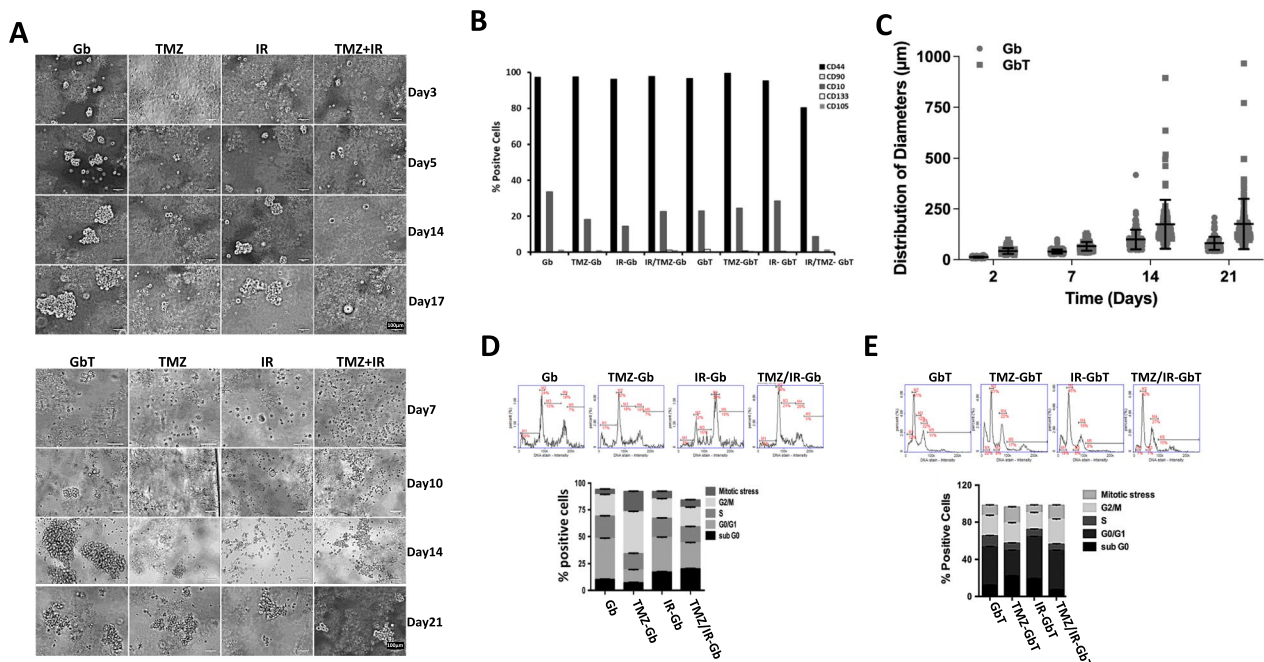


Fig. 2 Proliferation, survival upon TMZ ± IR of bioprinted MSC/GBM **A**) Cells extracted from scaffold treated with TMZ ± 2 Gy (IR) for the period of times indicated were grown under 3D conditions as described earlier [12]. Cells were collected 96 h after treatment (up to Day24 for co-cultures and Day17 for mono-cultures). Photos of cells in culture after 30 days post-treatment, which were used for RNA sequencing as described in materials and methods. **B**) MSC and GBM cell markers analyzed by FACS as described in Materials and Methods [10]. **C**) Cell proliferation was measured using diameters of the spheroids at the different times indicated in monoculture of GBM (Gb) and in co-cultures MSC/GBM (GbT). Cell cycle status analyzed by FACS as described in Materials and methods to determine the proportion of cells in the different cell cycle phases in untreated or treated Gb **(D)** and GbT **(E)**

expressed genes in pairwise comparison under the following conditions:

1. GbT (GBM+MSC^{CAF} tumoroid): vs. TMZ-GbT (50 μM TMZ treated GbT).
2. GbT vs. IR-GbT (2 Gy radiated GbT).
3. GbT vs. TMZ/IR-GbT (50 μM TMZ + 2 Gy treated GbT).
4. Gb (GBM tumoroid) vs. TMZ-Gb (50 μM TMZ treated Gb).
5. Gb vs. IR-Gb (2 Gy radiated Gb).
6. Gb vs. TMZ/IR-Gb (50 μM TMZ + 2 Gy radiated Gb).
7. Gb vs. GbT.
8. TMZ-Gb vs. TMZ-GbT.
9. IR-Gb vs. IR-GbT.
10. TMZ/IR-Gb vs. TMZ/IR-GbT.

The filter condition was a p-value with a cut-off of 0.1 or a shrunken log-fold change of 0.3. Genes meeting the screening criteria were defined as up-regulated differential gene when the log fold change was positive and down-regulated with a negative log change. As illustrated in Fig. 3A, the ration of genes up- or

down-regulated was similar under all condition but with different amplitude in gene numbers. TMZ was a more powerful inducer of differential gene expression than IR. Interestingly, the radiation of Gb at 2 Gy (Gb vs. IR-Gb) did not significantly alter the transcriptomes while it was more effective on GbT. Principle component (PC) analysis showed preferential clustering of Gb vs. GbT and a minor impact of 2 Gy on the transcriptome (Fig. 3B). As illustrated in Fig. 3C, the overall gene counts were increased in GbT compared to Gb and this mainly in TMZ-treated samples. In the latter case, it appears that in the top 10 genes expressed, 9 were mitochondrial DNA encoded (ND4, COX1, COX2, COX3, ATP6, CYB, NRN2, ND2, ND1) and one was an actin isoform (ACTB) (Fig. 3C insert). The cellular heterogeneity of GBM has been shown to affect its response to treatments and to promote a change in tumor phenotype/subtype [21]. We analyzed the main markers of classical, proneural and mesenchymal GBM subtypes [22, 23] in treated or untreated Gb and GbT. Of note, in this study the cultures were derived from a GBM characterized as mesenchymal subtype [24]. However, neither the co-culture with MSC^{CAF}(GbT)

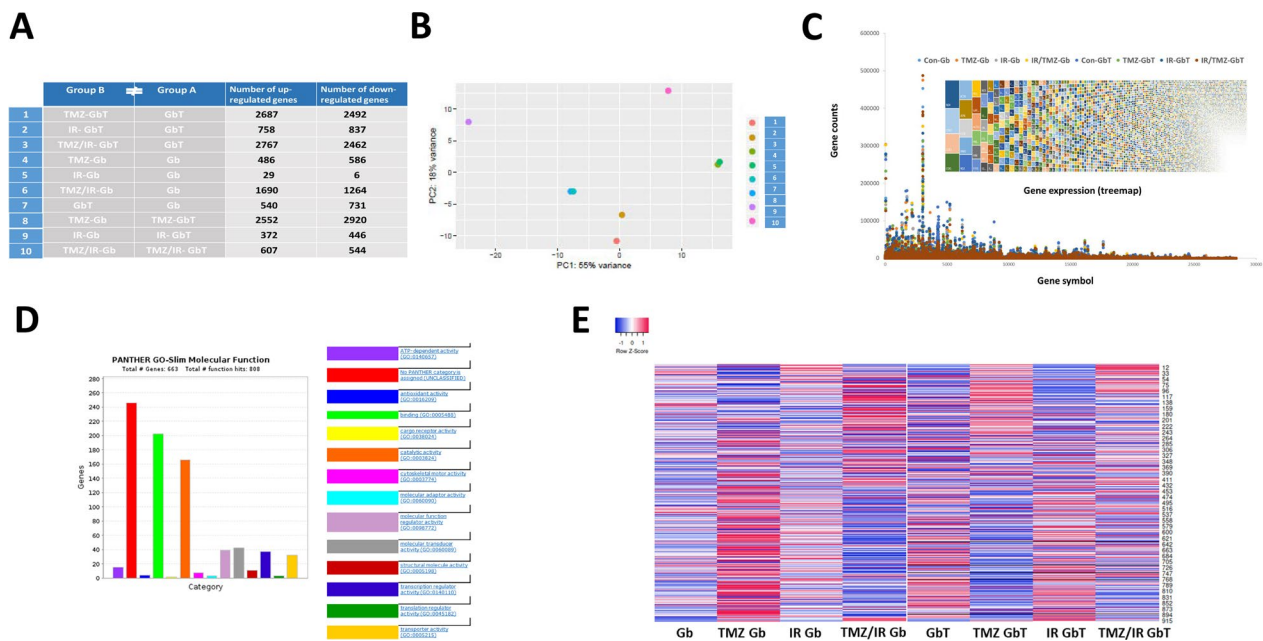


Fig. 3 Gene expression upon co-culture of MSC/GBM and therapeutic-like treatments **A**) Number of up- and down-regulated genes per pairwise comparison under the different conditions. **B**) Low dimensional embedding by Principal Components Analyses (PCA) of all samples. **C**) Representation of genes expression (identified and quantified by RNA-seq) in treated or untreated Gb and GbT with a Treemap representation of the most expressed genes (insert). **D**) Panther Gene ontology analysis of top expressed 915 genes. **E**) Heatmap of the top 915 expressed genes in treated or untreated Gb and GbT (clustering method: centroid ranking and distance measurement method, Spearman rank correlation)

nor the different treatments (TMZ, IR or TMZ + IR) affected the mesenchymal subtype classification of the tumor and/or promoted the emergence of a different GBM subtype (Figure S1). The analysis the expression of the most expressed genes between Gb and GbT (Table S1) using the PANTHER GO software showed that the main molecular functions represented in the top expressed genes belonged to several molecular pathways that were implicated into different biological functions; the majority of which were not categorized (Fig. 3D). Heatmaps of the top 900 signature genes under the different conditions confirmed that TMZ treatment induced a significant change in the differential gene hierarchical signature in Gb (Fig. 3E). On the other hand, radiation did not drastically affect the top gene signature (Fig. 3E). However, the transcriptomic landscape in TMZ-Gb appeared to be modified by radiation (compare TMZ-Gb vs. TMZ/IR-Gb). In GbT, again TMZ seemed to have the most effective consequence on gene expression while the combination of TMZ + IR promoted a unique signature. Of note, IR alone seem to induced a moderate change in the transcriptome in GbT (Fig. 3E). The presence of MSC^{CAF} in the co-cultures appeared to strongly modify the transcriptomic arrays of TMZ-treated or IR-treated GBM

but to a lesser degree that of the combined TMZ + IR-treated GBM (Fig. 3E).

Difference Analysis of top genes differentially expressed upon treatments in Gb and GbT

From the top 915 overexpressed genes, we extracted the 20 top over-expressed or top under-expressed genes. Figure 4A showed that these top differentially expressed genes belonged to multiple pathways with, nonetheless, an over-representation of mitochondrial genes belonging to several oxidative phosphorylation complexes (i.e. ATP8/Complex V, ND4L, ND5/complex I) were down-regulated in GbT while other mitochondrial genes were up-regulated (i.e. GLDC and MRPL33) (Fig. 4B). Of note, the effect of the treatments on the expression of these top differential expressed genes appeared to be less pronounced in monoculture (Gb) than in co-culture (GbT) (Fig. 4B, C). To obtain a better insight into the phenotype differences between Gb and GbT, we used Gene Ontology analysis, to further investigate pathways that could be potentially affected by the different treatments. Gene set enrichment analysis (GSEA) was performed on the input gene obtained by RNA-seq with a false discovery response (FDR) set at less than 5%. As shown in Fig. 4D, enrichment plot showed a few significant enrichments between Gb and GbT, with a positive association with

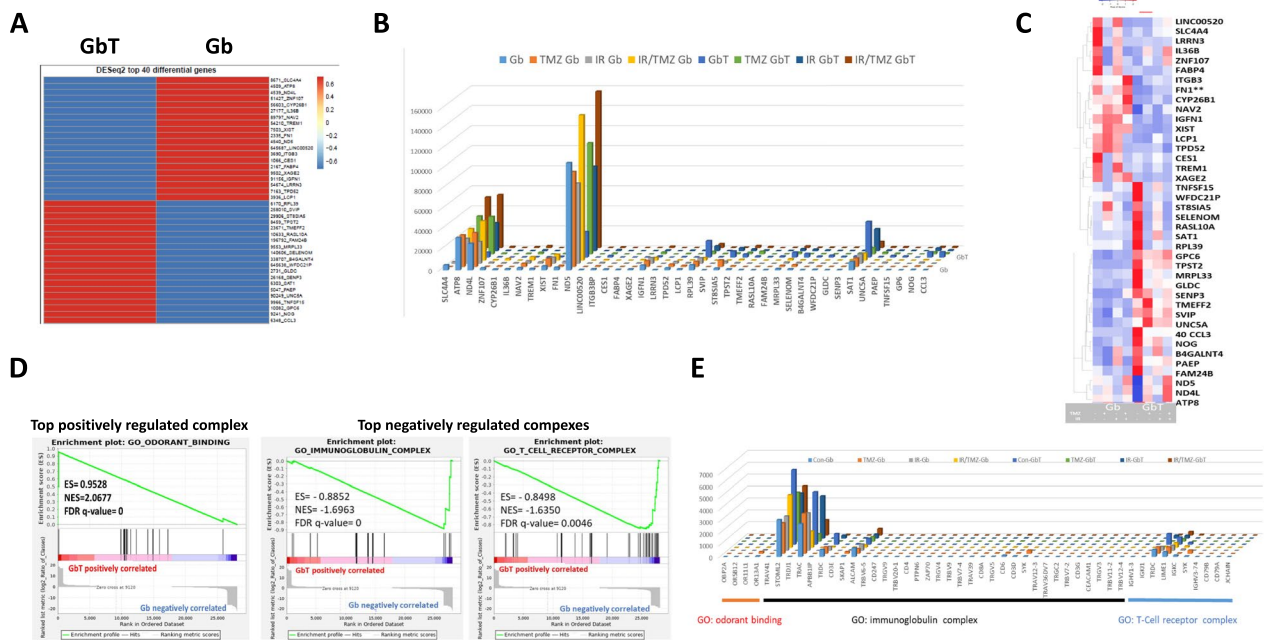


Fig. 4 Top gene expression in GBM mono- and co-culture with MSC **A**) Heatmap of the top 20 over- or 20 down-expressed genes in Gb vs. GbT. **B**) Gene counts of top genes over- or under-expressed in Gb vs. GbT under treated or untreated conditions. **C**) Heatmap of the top differentiated genes in untreated or treated Gb or GbT (clustering method: centroid ranking and distance measurement method, Spearman rank correlation). **D**) GSEA representation for the significantly up-regulated or down-regulated pathways for Gene Ontology database in the comparison of Gb and GbT. **E**) Histograms of gene counts of GSEA positively or negatively regulated between Gb and GbT

the “odorant binding complex” and a negative association with the production of immunoglobulins and the T cell receptor complex. A list of genes can be found in Fig. 4E. Of note, when the top positively or negatively regulated gene counts were analyzed (Fig. 4E), most of the genes appeared to exhibit counts too low to be taken into consideration with the exception of *STOML2*, a mitochondrial protein associated with T-cell activation as shown by Kirchof et al. [29], *TRAC* (T-cell Receptor *Alpha* Constant) and, to a lesser extent, *TRDC* (T Cell Receptor *Delta* Constant) and *ALCAM* (Activated Leukocyte Cell Adhesion Molecule), all members of the immunoglobulin receptor family. These results suggest that the co-culture of *MSC^{CAF}* with GBM impacts the response to chemotherapy mostly by modulating the expression of immunological receptors and mitochondrial functions. The role of odorant binding genes needs to be further evaluated although *OBP2A* has been implicated in cancer progression mainly based on RNA-seq data [30].

Impact of co-cultures on key GBM features and miRNA genes.

Cancer stem cells are thought to be the cornerstone of both the growth and resistance to therapy in GBM [25]. Analyses of stemness markers [26, 27] showed that the most common markers were unaffected by co-culture

and/or treatment with the exception of *Sox-2*, which was slightly increased in treated GbT while *nestin* was decreased under the same conditions (Fig. 5A). Of note, both the GbT and IR-GbT showed an increased expression of *L1-CAM*, a neural adhesion molecule, which has been implicated in GBM growth and migration [28]. Taken together our results suggest that the co-culture of GBM with *MSC^{CAF}* profoundly modify the transcriptomic landscape of the tumor but did not affect the molecular subtype although it impacted moderately the cancer stem cells profile. However, it is coherent with the fact that the treatments (*TMZ ± IR*) increased some cancer stem cells and mesenchymal subtypes markers. GBM are characterized by extensive angiogenesis, which requires the coordinated expression of genes with multiple families such as growth factors, metalloproteases, matrix components [31]. We used gene counts data to analyze the expression of angiogenesis related key genes in our co-cultures. As illustrated in Fig. 5B, *VEGFA* and *VEGFB* were highly expressed under our conditions and *VEGFA* appeared to be upregulated by treatment in both Gb and GbT. Similarly, the metalloproteases *MMP2* and *MMP14* and their cognate inhibitors *TIMP2* and *TIMP3* were also overexpressed and differently affected by the treatments in Gb and GbT. Of note, we found that collagen type 6 (both isoform *COL6A1* and *COL6A2*) was

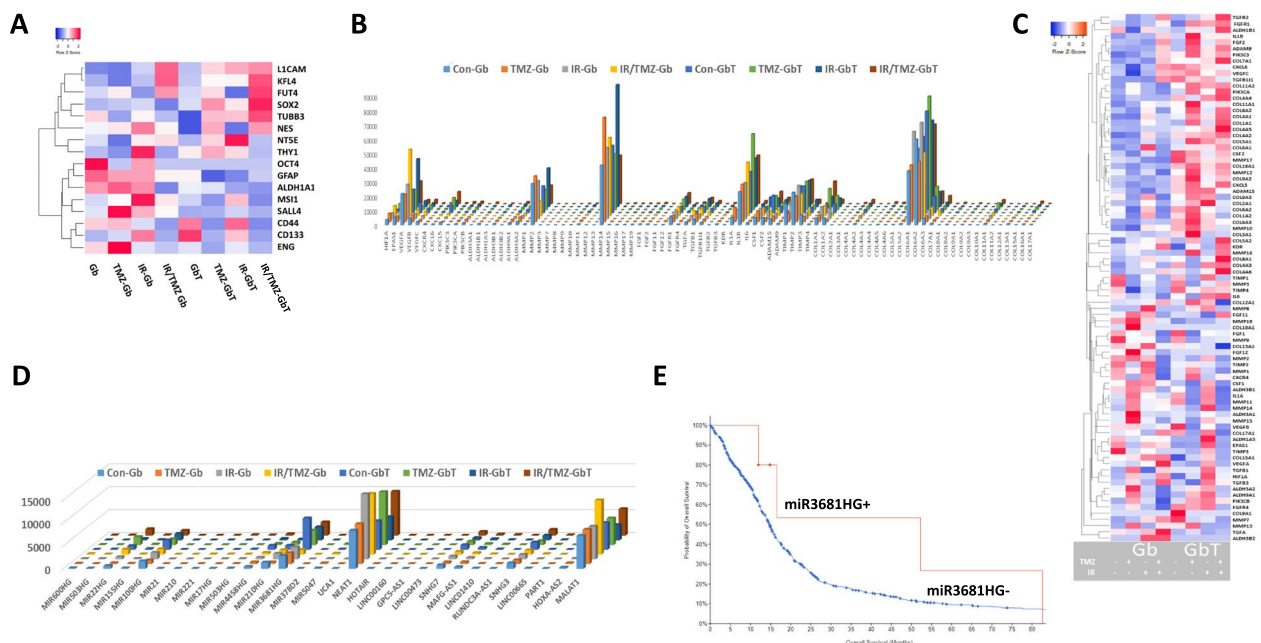


Fig. 5 Expression of cancer stem cells, angiogenesis related genes and miRNAHG in Gb and GbT **A**) Histograms of the GBM cancer stem cells marker genes in untreated or treated Gb and GbT (clustering method: centroid ranking and distance measurement method, Spearman rank correlation). **B**) Gene counts of angiogenesis-related genes expressed in untreated or treated Gb and GbT. **C**) Heatmap of the previous angiogenesis listed genes in untreated or treated Gb and GbT (clustering method: centroid ranking and distance measurement method, Spearman rank correlation). **D**) Gene counts of top miRNA host genes expressed in Gb and GbT. **E**) TCGA glioblastoma database analysis (23) on the influence of the expression of miR3681HG on GBM patient overall survival

overexpressed in Gb and GbT with a higher level of expression in GbT (Fig. 5B). Heatmap of the genes listed in Fig. 5B, showed that GbT exhibited, as expected, an invasion/angiogenesis profile different from Gb and that treatment (especially IR) acutely affected the expression of the implicated genes (Fig. 5C).

Recently, it has been shown that non-coding genes such as miRNA play an important role in the regulation of angiogenesis and other major characteristics of GBM [32, 33]. We examined the expression of miRNA-host genes under our conditions and as illustrated in Fig. 5D, few miRNA were significantly expressed. It should be noted that due to the RNA sequencing process, we did not have access to small miRNAs. However, miR3681HG, which belongs to the lncRNA class, appeared to be differentially expressed in Gb vs. GbT. The expression of miR3681HG is associated with a longer survival of GBM patients (Fig. 5E), which suggests an effect on GBM progression in clinical situations.

Chromatin remodeling in Gb and GbT

GBM are characterized by chromatin remodeling during its evolution under treatments [34, 35]. We performed genome-wide profiling of open chromatin by ATAC-seq (Assay for Transposase-Accessible Chromatin with high throughput sequencing). Average ATAC-seq signal at

Merged Regions (= all peak regions), transcription start sites (TSS) and gene bodies were plotted. ATAC-seq data were also presented as Heatmaps in which the data are clustered (indicated by C1-C5). This analysis was completed with RNA-seq analysis to find the significant differences between treated and untreated Gb and GbT with the expectation that co-culture and/or TMZ could modify chromatin accessibility, which in turn, could result in the differential expressed of specific genes. As shown in Fig. 6A, very little differences were observed between chromatin accessibility in Gb or GbT control or treated with TMZ. PCA of TMZ-treated or untreated Gb or GbT indicated no clear clustering between Gb and GbT (Fig. 6B). We completed this study by analyzing the gene counts of the key epigenetic actors. As illustrated in Fig. 6C, the main differences between Gb and GbT was an increase in MBD2 and a decrease in KDM5C; 2 factors that are implicated in poor prognosis in GBM [36, 37]. For both enzymes, gene expression was not drastically altered by TMZ and/or IR (Fig. 6C).

RNA-seq indicated several significant changes due to chromatin remodeling induced by the co-culture of GBM with MSC^{CAF}, GNAL1 expression was reduced in Gb vs. GbT while that of NRXN1 was increased (Table 1). Of note, the regulation of GALN1 that encodes for the stimulatory G protein *alpha* subunit, which mediates

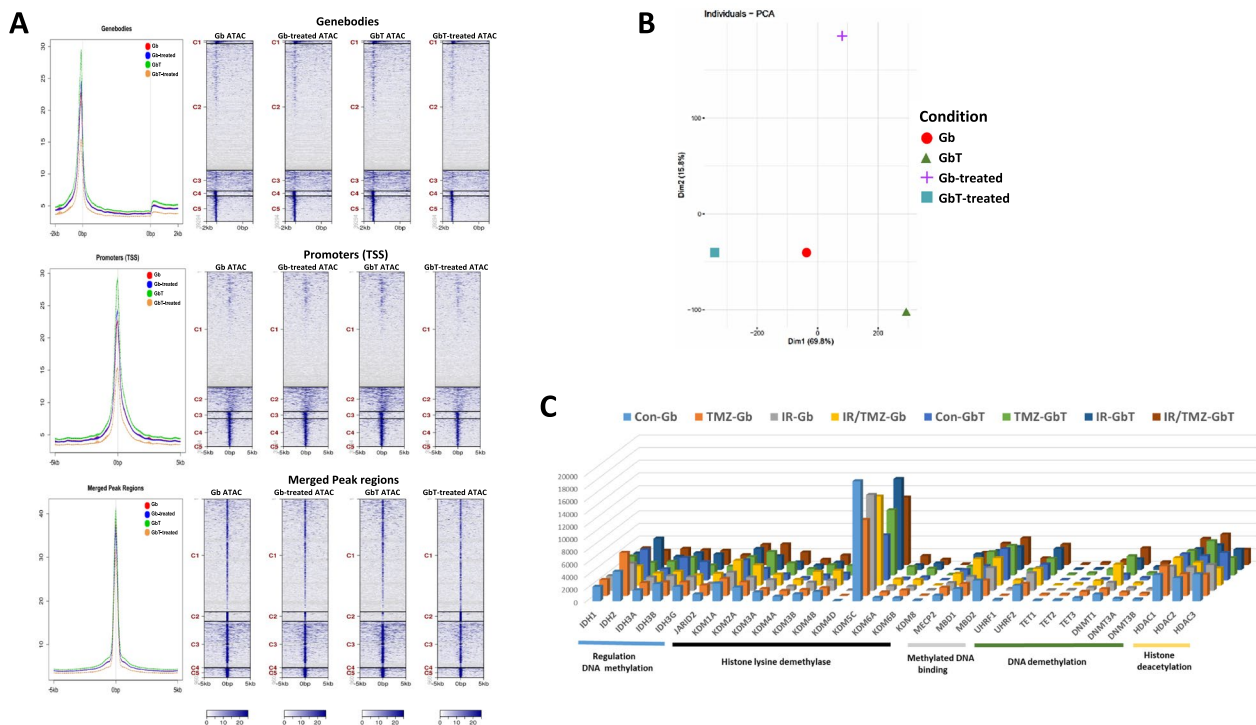


Fig. 6 ATAC-seq analyses of GBM monoculture vs. MSC/GBM co-culture **A** The average read density (right) and heatmaps (left) indicating ATAC-seq signal across a genomic window of upstream -5 kb to +5 kb downstream of different regions (i.e. gene bodies, promoter and merged peak regions) of untreated or TMZ-treated Gb and GbT. **B** PCA analysis of Gb and GbT treated or not with TMZ. **C** Expression of key genes implicated in epigenetic regulation

odorant signaling, is in agreement with the GSEA analyses illustrated in Fig. 4D. NRXN1, which is mainly expressed in the vertebrate nervous system and acts as a cell adhesion molecule and receptor, has no identified function in GBM. TMZ treatment had a drastic effect on chromatin remodeling differential gene expression with several genes, belonging to a wide spectrum of cellular functions, affected in GbT (Fig. 7A). On the other hand, only two genes were affected by TMZ treatment in Gb; TNFRSF-11 (TNF receptor superfamily member 11b) and TREM-1 (Triggering receptor expressed on myeloid cells 1). TNFRSF-11 is also known as osteoprotegerin and inhibits TRAIL (TNF-related apoptosis-inducing ligand) induced apoptosis in both normal and tumor cells [38]. TREM-1 is a member of the immunoglobulin superfamily transmembrane protein, which has been associated with enhanced tumor grade and poor patient outcome in numerous types of cancers including GBM [39]. Bioportal analysis indicates that TREM-1 expression in GBM is associated with shorter survival (Fig. 7B). Of note, the expression of TREM-1 appears to be the most epigenetically-regulated gene in both Gb and GbT after TMZ treatment (Fig. 7C). The TREM-1 signaling pathway is associated with inflammatory cancers and is an

amplifier of immune responses [40]. The expression level of TREM-1 has been shown to be significantly increased in GBM [41] and interacted mostly with a soluble ligand to activate membrane-bound DAP12 to induce PI3K and GRB2 signaling pathways [42]. We used the RNA-seq gene counts to monitor both the expression of TREM-1 ligands (i.e. HMGB1, PGLYRP1, HSPA1A, and CIRBP) and intracellular signaling (DAP12, ZAP70, Syk, PI3K, GRB2, SOS1 and SOS2). As shown in Fig. 7D, none of the genes encoding for TREM-1 interacting partners appears to follow TREM-1 differential expression in Gb and GbT as well as between Gb and TMZ-Gb. We did not find any expression of TREM-2 or other members of the TREM family in our RNA seq data (**not shown**).

Discussion

The origin and the roles of MSC in GBM remain ill-defined although they are implicated at several levels during gliomagenesis and its progression under treatment but the exact mechanisms underlying their function in cancer are unknown [7, 43]. In previous works, we have developed a 3D biosphere model to study the interaction between MSC and GBM and showed that in contact with GBM, MSC were transformed to CAF

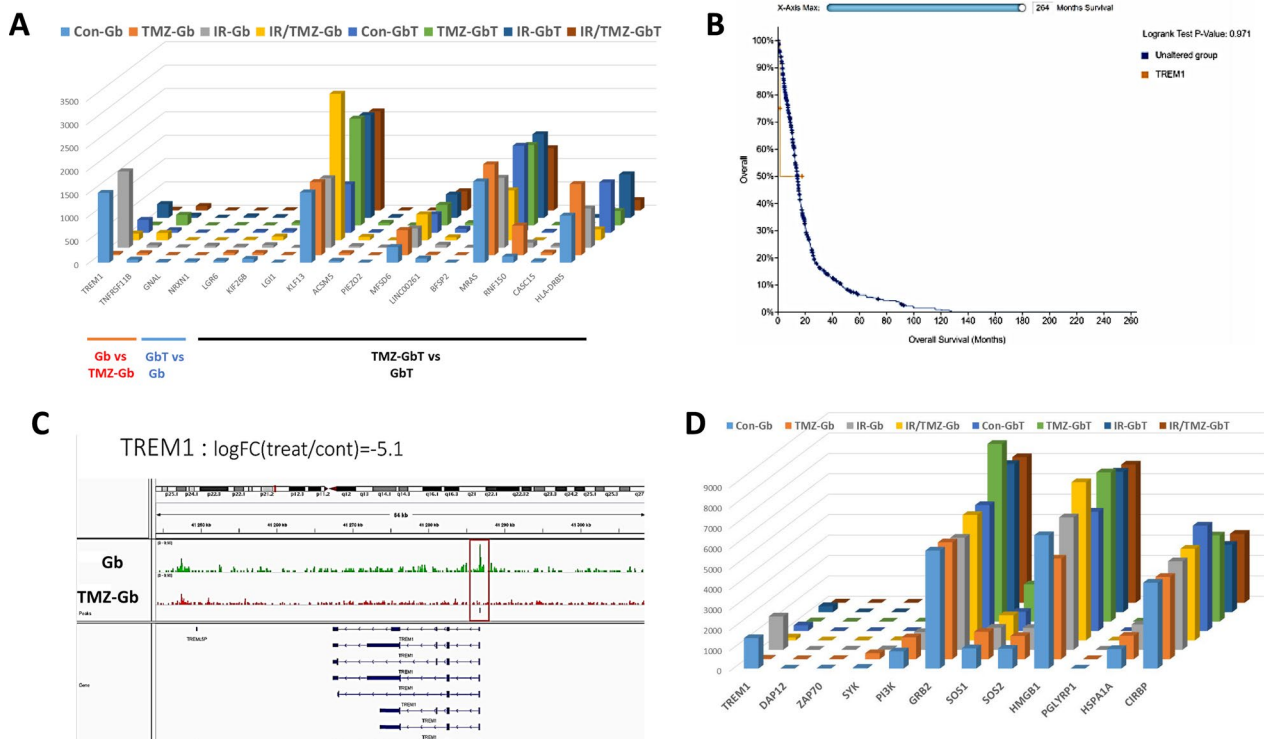


Fig. 7 TREM-1 differential epigenetic regulation in GBM versus MSC/GBM cultures **A**) Genes expressed from simultaneous profiling of DNA accessibility and Gene expression dynamics with ATAC-Seq and RNA-Seq. **B**) Impact of TREM-1 on the overall survival of GBM patients (TCGA data, ref 23). **C**) Epigenetic profiling of TREM-1 gene in Gb and TMZ-Gb. **D**) Gene counts for key genes implicated in TREM-1 function

we called here MSC^{CAF} [10–12]. We demonstrated that MSC^{CAF} promoted GBM survival through mitochondrial exchanges in co-cultures [10]. Nonetheless, MSC are attractive therapeutic targets and thus more relevant models are needed to evaluate their roles as potential anticancer targets [44].

In the present work, we used a 3D scaffold model obtained with bioprinted GBM/MSC^{CAF} co-cultures, treated or not with conventional glioma therapies (chemo- and/or radio-therapy), to analyze at the transcriptomic level the impact of human bone derived human MSC on GBM (Fig. 1, 2). Of interest, mitochondrial DNA encoded genes were the top expressed genes emphasizing the importance of mitochondria in the MSC/GBM interactions under 3D culture conditions (Fig. 3). The transcriptomic differences observed between Gb and GbT in the top 900 expressed genes encompass several pathways (Fig. 3). Of note, in Gb, TMZ has a profound effect on the expression of the top genes, which were modulated by the combination with IR, but as a single agent did not affect the transcriptome (Fig. 3). This implies that the combination treatment is more reliable to the actual patients’ situation. The addition of MSC^{CAF} also alter the transcriptional landscape compared to Gb as well as its response to treatment. The

co-culture GBM/MSC^{CAF} did not affect a specific pathway but rather modified the major cellular constitutive processes (Fig. 3B, C). Quite interestingly, neither the MSC^{CAF} and/or therapy modify the cancer stem cell signatures (Fig. 3D). Interestingly, several genes implicated in mitochondrial and immune related genes are present in the top 40 genes differentially expressed in Gb vs. GbT (Figs. 3, 4). This is consistent with the central role mitochondria play in the interactions between cancer and the microenvironment and the organelle exchanges observed between MSC and GBM in vitro [3, 4]. The analysis of the genes implicated in angiogenesis (Fig. 5A, B) indicated that the co-culture of MSC^{CAF} and GBM affect the expression of several key genes such as CXCL5 and COL16A, which has been associated with GBM invasiveness, tumorigenesis and angiogenesis [45, 46]. To further study the influence of MSC^{CAF} on GBM, we focused on the expression of miRNA and as illustrated in Fig. 6C, we found that one lncRNA (miR3681HG) is differentially expressed in Gb and GbT. Very little information is available on miR3681HG in cancer. However, its expression is associated with longer overall survival in GBM patients (Fig. 5D) (Table 1)

The TME and/or therapy are implicated in the chromatin remodeling in GBM [3, 4], in fact we observed a

Table 1: Genes expression regulated by chromatin remodeling in treated and untreated Gb and GbT. List of genes up- or down-regulated by epigenetic regulation as obtained by RNA-seq after ATAC-seq analyses described in Materials and Methods.

| | Gb | GbT |
|---------|------------------------|---|
| Gb | X | ↓ GNAL1 ↑ NRXN1 |
| TMZ-Gb | ↓ TREM1 ↑ TNFRSF11b | na |
| GbT | ↑ GNAL1 ↓ NRXN1 | X |
| TMZ-GbT | na | ↑ LGR6, KIF26B, LGI1, KLF13, ACSM5, PIEZO2, MFSD6, LINC00261, BFPSP2, MRAS, RNF150, CASC15, HLADRB5 |

limited effect of TMZ and/or co-culture with MSC^{CAF} in our models. However, among the limited number of genes affected by chromatin changes (Fig. 7A), we focused on TREM-1, which belongs to the Ig-like superfamily and is mainly found expressed on myeloid cells and recently observed in the TME of GBM where it plays an important role in GBM progression [47]. We found that TREM-1 is expressed in Gb more than in GbT and is downregulated by TMZ (Fig. 3A) and is down-regulated by TMZ and/or irradiation (Fig. 7A). However, we did not observe any change in the intracellular effectors and ligands of TREM-1, at least at a transcriptional level (Fig. 7D).

Little is known about the role of miR3681HG in cancer. On the other hand, it has been shown that TREM-1 deficiency globally remodels the TME toward an immune-permissive state [48]. Thus, further studies based on pharmacological intervention needed to be conducted, such as inhibition of TREM-1 activity by LP17.

Conclusion

Taken together, our study has established that bioprinted GBM/MS^{CAF} co-culture is feasible and has revealed potential new targets in GBM. However, further studies using relevant animal and cellular models are needed to assess the role of TREM-1 and miR3681HG in GBM and especially the role of MS^{CAF} and TMZ in the epigenetic regulation of TREM-1.

Abbreviations

| | |
|----------|--|
| ATAC seq | Assay for Transposase Accessible Chromatin with high throughput sequencing |
| CAF | Cancer-associated fibroblasts |
| CM | GBM conditioned defined medium |

| | |
|-------------------|--|
| DM | Defined Medium |
| GBM | Glioblastoma |
| Gb | Glioblastoma bioprinted tumoroid |
| GbT | Glioblastoma plus CAF bioprinted tumoroid |
| IR | Ionizing Radiation |
| LncRNA | Long non-coding RNA |
| MSC | Mesenchymal Stem Cells |
| MS ^{CAF} | MSC activated by conditioned media from GBM cultures |
| RNA seq | RNA sequencing |
| TME | Tumor Microenvironment |
| TMZ | Temozolomide |
| TREM-1 | Triggering Receptor Expressed on Myeloid cells 1 |

Supplementary Information

The online version contains supplementary material available at <https://doi.org/10.1186/s13287-024-04022-6>.

Additional file 1.

Acknowledgements

we thank the platform MicroPicell for their aid with all the microscopic work expert technical assistance.

Author contributions

LO performed experiments with 3D bioprinting models; CG performed Q-PCR complementary experiments. AS revised the bioinformatics data provided by active motive and performed additional analyses with YL; FP and DH critically revised the manuscript; FMV collected data for the preparation of figures and wrote the main manuscript text with LO and AS. All authors have read and agreed to the published version of the manuscript.

Funding

This work is supported by grants from "Ligue Grand Ouest Contre le Cancer (grant number RN19040NN) and the "Plan Cancer HTE program MoGImaging" (grant number: HTE C16073NS),

Availability of data and material

Most data generated or analyzed during this study are included in this article. The datasets and materials used and/or analyzed during the current study are available from the corresponding author on reasonable request. The RNA-seq/ATAC-seq data are available in European Nucleotide Archive with the accession number PRJEB76177.

Declarations

Ethics approval and consent to participate

The bio-collection used for this analysis is the Glioblastoma collection belonging to the approved project, "pediatric research program of the University Hospital of Nantes, France (Ref. MESR DC-2014–2206)", having obtained an institutional approval from committee patients protection board, "CPP Ouest IV, approval number "Dossier 06/15", date of approval 08/04/2015. The patients or their guardians/legally authorized representatives/next of kin provided written informed consent for participation in the use of samples. After informed consent, tumor samples classified as GBM, based on the World Health Organization criteria, were obtained from patients undergoing surgical intervention at the Department of Neurosurgery at "Centre Hospitalier Universitaire de Nantes" and the "Tumorotheque IRCNA".

Declaration of use of AI

The authors declare that artificial intelligence is not used in this study.

Competing Interests

The authors declare that they have no competing of interest.

Received: 11 June 2024 Accepted: 28 October 2024

Published online: 14 November 2024

References

- Oronsky B, Reid TR, O'Cransky A, Sandhu N, Knox SJ. A review of newly diagnosed Glioblastoma. *Front Oncol*. 2021;10:574012. <https://doi.org/10.3389/fonc.2020.574012>. (PMCID: PMC7892469).
- Stupp R, Mason WP, van den Bent MJ, Weller M, Fisher B, Taphoorn MJ, Belanger K, Brandes AA, Marosi C, Bogdahn U, Curschmann J, Janzer RC, Ludwin SK, Gorlia T, Allgeier A, Lacombe D, Cairncross JG, Eisenhauer E, Mirimanoff RO; European Organisation for Research and Treatment of Cancer Brain Tumor and Radiotherapy Groups; National Cancer Institute of Canada Clinical Trials Group. Radiotherapy plus concomitant and adjuvant temozolomide for glioblastoma. *N Engl J Med*. 2005 Mar 10;352(10):987–96. <https://doi.org/10.1056/NEJMoa043330>. PMID: 15758009.
- Bikfalvi A, da Costa CA, Avril T, Barnier JV, Bauchet L, Brisson L, Cartron PF, Castel H, Chevet E, Chneiweiss H, Clavreul A, Constantin B, Coronas V, Daubon T, Dontenwill M, Ducray F, Enz-Werle N, Figarella-Branger D, Fournier I, Frenel JS, Gabut M, Galli T, Gavard J, Huberfeld G, Hugnot JP, Idbah A, Junier MP, Mathivet T, Menei P, Meyronet D, Mirjolet C, Morin F, Mosser J, Moyal EC, Rousseau V, Salzet M, Sanson M, Seano G, Tabouret E, Tchoghadjian A, Turchi L, Vallette FM, Vats S, Verreault M, Virolle T. Challenges in glioblastoma research: focus on the tumor microenvironment. *Trends Cancer*. 2023 Jan;9(1):9–27. <https://doi.org/10.1016/j.trecan.2022.09.005>. Epub 2022 Nov 16. Erratum in: *Trends Cancer*. 2023 Aug;9(8):692. PMID: 36400694.
- Oliver L, Laliere L, Salaud C, Heymann D, Cartron PF, Vallette FM. Drug resistance in glioblastoma: are persisters the key to therapy? *Cancer Drug Resist*. 2020;3:287–301. <https://doi.org/10.20517/cdr.2020.29>. (PMCID: PMC8992484).
- Sundar SJ, Shakya S, Barnett A, Wallace LC, Jeon H, Sloan A, Recinos V, Hubert CG. Three-dimensional organoid culture unveils resistance to clinical therapies in adult and pediatric glioblastoma. *Transl Oncol*. 2022, 15:101251. <https://doi.org/10.1016/j.tranon.2021.101251>. Epub 2021 Oct 23. PMID: 34700192; PMCID: PMC8551697.
- Behnan J, Isakson P, Joel M, Cilio C, Langmoen IA, Vik-Mo EO, Badn W. Recruited brain tumor-derived mesenchymal stem cells contribute to brain tumor progression. *Stem Cells*. 2014;32:1110–23. <https://doi.org/10.1002/stem.1614>. (PMID: 24302539).
- Bajetto A, Thellung S, Dellacasa grande I, Pagano A, Barbieri F, Florio T. Cross talk between mesenchymal and glioblastoma stem cells: Communication beyond controversies. *Stem Cells Transl Med*. 2020;9(11):1310–30. <https://doi.org/10.1002/sctm.20-0161>.
- Shahar T, Rozovski U, Hess KR, Hossain A, Gumin J, Gao F, Fuller GN, Goodman L, Sulman EP, Lang FF. Percentage of mesenchymal stem cells in high-grade glioma tumor samples correlates with patient survival. *Neuro Oncol*. 2017;19(5):660–8. <https://doi.org/10.1093/neuonc/nov239>. (PMCID: PMC5464439).
- Clavreul A, Menei P. Mesenchymal stromal-like cells in the Glioma micro-environment: What are these cells? *Cancers (Basel)*. 2020;1512(9):2628. <https://doi.org/10.3390/cancers12092628>. (PMCID: PMC7565954).
- Salaud C, Alvarez-Arenas A, Geraldo F, Belmonte-Beitia J, Calvo GF, Gratas C, Pecqueur C, Garnier D, Pérez-García V, Vallette FM, Oliver L. Mitochondria transfer from tumor-activated stromal cells (TASC) to primary Glioblastoma cells. *Biochem Biophys Res Commun*. 2020;533(1):139–47. <https://doi.org/10.1016/j.bbrc.2020.08.101>. (Epub 2020 Sep 15 PMID: 32943183).
- Garnier D, Ratcliffe E, Briand J, Cartron PF, Oliver L, Vallette FM. The activation of mesenchymal stem cells by glioblastoma microvesicles alters their exosomal secretion of miR-100-5p, miR-9-5p and let-7d-5p. *Biomedicines*. 2022;10(1):112. <https://doi.org/10.3390/biomedicines10010112>. (PMCID: PMC8773192).
- Oliver L, Álvarez-Arenas A, Salaud C, Jiménez-Sánchez J, Calvo GF, Belmonte-Beitia J, Blandin S, Vidal L, Pérez V, Heymann D, Vallette FM. A Simple 3D cell culture method for studying the interactions between human mesenchymal stromal/stem cells and patients derived glioblastoma. *Cancers (Basel)*. 2023;15:1304. <https://doi.org/10.3390/cancers15041304>. (PMCID: PMC9954562).
- Jubelin C, Muñoz-García J, Gríscom L, Cochonneau D, Olivier E, Heymann MF, Vallette FM, Oliver L, Heymann D. Three-dimensional in vitro culture models in oncology research. *Cell Biosci*. 2022;12:155. <https://doi.org/10.1186/s13578-022-00887-3>. (PMCID: PMC9465969).
- Jubelin C, Muñoz-García J, Cochonneau D, Olivier E, Vallette F, Heymann MF, Oliver L, Heymann D. Technical report: liquid overlay technique allows the generation of homogeneous osteosarcoma, glioblastoma, lung and prostate adenocarcinoma spheroids that can be used for drug cytotoxicity measurements. *Front Bioeng Biotechnol*. 2023;11:1260049. <https://doi.org/10.3389/fbioe.2023.1260049>. (PMID: 37869710).
- Weiswald LB, Bellet D, Dangles-Marie V. Spherical cancer models in tumor biology. *Neoplasia*. 2015;17(1):1–15. <https://doi.org/10.1016/j.neo.2014.12.004>. PMID: 25622895; PMCID: PMC4309685.
- Leong SW, Tan SC, Norhayati MN, Monif M, Lee SY. Effectiveness of bioinks and the clinical value of 3D Bioprinted glioblastoma models: a systematic review. *Cancers (Basel)*. 2022;14(9):2149. <https://doi.org/10.3390/cancers14092149>. PMID: 35565282; PMCID: PMC9103189.
- Pasupuleti V, Vora L, Prasad R, Nandakumar DN, Khatri DK. Glioblastoma preclinical models: Strengths and weaknesses. *Biochim Biophys Acta Rev Cancer*. 2024 Jan;1879(1):189059. <https://doi.org/10.1016/j.bbcan.2023.189059>. Epub 2023 Dec 16. PMID: 38109948.
- Brocard E, Oizel K, Laliere L, Pecqueur C, Paris F, Vallette FM, Oliver L. Radiation-induced PGE2 sustains human glioma cells growth and survival through EGF signaling. *Oncotarget*. 2015;6(9):6840–9. <https://doi.org/10.18632/oncotarget.3160>. (PMID: 25749386).
- Buenrostro JD, Giresi PG, Zaba LC, Chang HY, Greenleaf WJ. Transposition of native chromatin for fast and sensitive epigenomic profiling of open chromatin, DNA-binding proteins and nucleosome position. *Nat Methods*. 2013;10(12):1213–8. <https://doi.org/10.1038/nmeth.2688>. (Epub 2013 Oct 6 PMID: 24097267).
- Corces MR, Trevino AE, Hamilton EG, Greenside PG, Sinnott-Armstrong NA, Vesuna S, Satpathy AT, Rubin AJ, Montine KS, Wu B, Kathiria A, Cho SW, Mumbach MR, Carter AC, Kasowski M, Orloff LA, Risco VI, Kundaje A, Khavari PA, Montine TJ, Greenleaf WJ, Chang HY. An improved ATAC-seq protocol reduces background and enables interrogation of frozen tissues. *Nat Methods*. 2017;14(10):959–62. <https://doi.org/10.1038/nmeth.4396>. (Epub 2017 Aug 28 PMID: 28846090).
- Eisenbarth D, Wang YA. Glioblastoma heterogeneity at single cell resolution. *Oncogene*. 2023 Jun;42(27):2155–2165. <https://doi.org/10.1038/s41388-023-02738-y>. Epub 2023 Jun 5. PMID: 37277603; PMCID: PMC10913075.
- Phillips HS, Kharbanda S, Chen R, Forrest WF, Soriano RH, Wu TD, Misra A, Nigro JM, Colman H, Soroceanu L, Williams PM, Modrusan Z, Feuerstein BG, Aldape K. Molecular subclasses of high-grade glioma predict prognosis, delineate a pattern of disease progression, and resemble stages in neurogenesis. *Cancer Cell*. 2006;9(3):157–73. <https://doi.org/10.1016/j.ccr.2006.02.019>. (PMID: 16530701).
- Verhaak RG, Hoadley KA, Purdom E, Wang V, Qi Y, Wilkerson MD, Miller CR, Ding L, Golub T, Mesirov JP, Alexe G, Lawrence M, O'Kelly M, Tamayo P, Weir BA, Gabriel S, Winckler W, Gupta S, Jakkula L, Feiler HS, Hodgson JG, James CD, Sarkaria JN, Brennan C, Kahn A, Spellman PT, Wilson RK, Speed TP, Gray JW, Meyerson M, Getz G, Perou CM, Hayes DN; Cancer Genome Atlas Research Network. Integrated genomic analysis identifies clinically relevant subtypes of glioblastoma characterized by abnormalities in PDGFRA, IDH1, EGFR, and NF1. *Cancer Cell*. 2010 Jan 19;17(1):98–110. <https://doi.org/10.1016/j.ccr.2009.12.020>. PMID: 20129251; PMCID: PMC2818769.
- Oizel K, Chauvin C, Oliver L, Gratas C, Geraldo F, Jarry U, Scotet E, Rabe M, Alves-Guerra MC, Teusan R, Gautier F, Loussouarn D, Compan V, Martinou JC, Vallette FM, Pecqueur C. Efficient Mitochondrial Glutamine targeting prevails over Glioblastoma metabolic plasticity. *Clin Cancer Res*. 2017;23(20):6292–304. <https://doi.org/10.1158/1078-0432.CCR-16-3102>. (Epub 2017 Jul 18 PMID: 28720668).
- Bao S, Wu Q, McLendon RE, Hao Y, Shi Q, Hjelmeland AB, Dewhirst MW, Bigner DD, Rich JN. Glioma stem cells promote radioresistance by preferential activation of the DNA damage response. *Nature*. 2006;444(7120):756–60. <https://doi.org/10.1038/nature05236>. (Epub 2006 Oct 18 PMID: 17051156).
- Lemke D, Weiler M, Blaes J, Wiestler B, Jestaedt L, Klein AC, Löw S, Eisele G, Radlwimmer B, Capper D, Schmieider K, Mittelbronn M, Combs SE, Bendszus M, Weller M, Platten M, Wick W. Primary glioblastoma cultures: can profiling of stem cell markers predict radiotherapy sensitivity? *J Neurochem*. 2014;131(2):251–64. <https://doi.org/10.1111/jnc.12802>. (Epub 2014 Jul 18 PMID: 24976529).
- Hattermann K, Flüh C, Engel D, Mehdorn HM, Synowitz M, Mentlein R, Held-Feindt J. Stem cell markers in glioma progression and recurrence.

- Int J Oncol. 2016;49(5):1899–910. <https://doi.org/10.3892/ijo.2016.3682>. (Epub 2016 Sep 6 PMID: 27600094).
28. Bradshaw A, Wickremsekera A, Tan ST, Peng L, Davis PF, Itinteang T. Cancer stem cell hierarchy in Glioblastoma multiforme. *Front Surg*. 2016;15(3):21. <https://doi.org/10.3389/fsurg.2016.00021>. (PMCID: PMC4831983).
 29. Bao S, Wu Q, Li Z, Sathornsumetee S, Wang H, McLendon RE, Hjelmeland AB, Rich JN. Targeting cancer stem cells through L1CAM suppresses glioma growth. *Cancer Res*. 2008;68(15):6043–8. <https://doi.org/10.1158/0008-5472.CAN-08-1079>. (PMCID: PMC2739001).
 30. Kirchof MG, Chau LA, Lemke CD, Vardhana S, Darlington PJ, Márquez ME, Taylor R, Rizkalla K, Blanca I, Dustin ML, Madrenas J. Modulation of T cell activation by stomatin-like protein 2. *J Immunol*. 2008;181(3):1927–36. <https://doi.org/10.4049/jimmunol.181.3.1927>. (PMID: 18641330).
 31. Chung C, Cho HJ, Lee C, Koo J. Odorant receptors in cancer. *BMB Rep*. 2022;55(2):72–80. <https://doi.org/10.5483/BMBRep.2022.55.2.010>. (PMCID: PMC8891625).
 32. Rosińska S, Gavard J. Tumor vessels fuel the fire in Glioblastoma. *Int J Mol Sci*. 2021;22(12):6514. <https://doi.org/10.3390/ijms22126514>. (PMID: 34204510).
 33. Song Z, Xue Z, Wang Y, Imran M, Assiri M, Fahad S. Insights into the roles of non-coding RNAs and angiogenesis in glioblastoma: An overview of current research and future perspectives. *Biochim Biophys Acta Gen Subj*. 2024;1868(4):130567. <https://doi.org/10.1016/j.bbagen.2024.130567>.
 34. Behrooz AB, Latifi-Navid H, Nezhadi A, Świat M, Los M, Jamalpoor Z, Ghavami S. Molecular mechanisms of microRNAs in glioblastoma pathogenesis. *Biochim Biophys Acta Mol Cell Res*. 2023;1870(6):119482. <https://doi.org/10.1016/j.bbamcr.2023.119482>. (PMID: 37146725).
 35. Wu Q, Berglund AE, Etame AB. The impact of epigenetic modifications on adaptive resistance evolution in Glioblastoma. *Int J Mol Sci*. 2021;22(15):8324. <https://doi.org/10.3390/ijms22158324>. PMID:34361090; PMCID:PMC8347012.
 36. Chen HM, Nikolic A, Singhal D, Gallo M. Roles of chromatin remodelling and molecular heterogeneity in therapy resistance in Glioblastoma. *Cancers (Basel)*. 2022;14(19):4942. <https://doi.org/10.3390/cancers14194942>. PMID:36230865;PMCID:PMC9563350.
 37. Zhu D, Hunter SB, Vertino PM, Van Meir EG. Overexpression of MBD2 in glioblastoma maintains epigenetic silencing and inhibits the antiangiogenic function of the tumor suppressor gene BAI1. *Cancer Res*. 2011;71(17):5859–70. <https://doi.org/10.1158/0008-5472.CAN-11-1157>. (PMID: 21724586).
 38. Drongitis D, Verrillo L, De Marinis P, Orabona P, Caiola A, Turitto G, Alfieri A, Bruscella S, Gentile M, Moriello V, Sannino E, Di Muccio I, Costa V, Miano MG, de Bellis A. The chromatin-oxygen sensor gene KDM5C associates with novel hypoxia-related signatures in Glioblastoma multiforme. *Int J Mol Sci*. 2022;23:10250.
 39. Wang Y, Liu Y, Huang Z, Chen X, Zhang B. The roles of osteoprotegerin in cancer, far beyond a bone player. *Cell Death Discov*. 2022;8:252.
 40. Zhang L, Qu X, Xu Y. Molecular and immunological features of TREM1 and its emergence as a prognostic indicator in glioma. *Front Immunol*. 2024;2(15):1324010. <https://doi.org/10.3389/fimmu.2024.1324010>. PMID: 38370418;PMCID:PMC10869492.
 41. Colonna M. The biology of TREM receptors. *Nat Rev Immunol*. 2023;23:580–94.
 42. Lu Q, Xie Y, Qi X, Yang S. TREM1 as a novel prognostic biomarker and tumor immune microenvironment evaluator in glioma. *Medicine (Baltimore)*. 2023;102(48):e36410. <https://doi.org/10.1097/MD.00000000000036410>. PMID:38050264;PMCID:PMC10695587.
 43. Arts RJ, Joosten LA, van der Meer JW, Netea MG. TREM-1: intracellular signaling pathways and interaction with pattern recognition receptors. *J Leukoc Biol*. 2013;93(2):209–15. <https://doi.org/10.1189/jlb.0312145>. (Epub 2012 Oct 29 PMID: 23108097).
 44. Nowak B, Rogujski P, Janowski M, Lukomska B, Andrzejewska A. Mesenchymal stem cells in glioblastoma therapy and progression: How one cell does it all. *Biochim Biophys Acta Rev Cancer*. 2021;1876(1):188582. <https://doi.org/10.1016/j.bbcan.2021.188582>.
 45. Zhang Q, Xiang W, Yi Dy, Xue Bz, Wen Ww, Abdelmaksoud A, Xiong Nx, Jiang Xb, Zhao Hy, Fu P. Current status and potential challenges of mesenchymal stem cell-based therapy for malignant gliomas. *Stem Cell Res Ther* 9, 228 (2018). doi.org/<https://doi.org/10.1186/s13287-018-0977-z>.
 46. Senner V, Ratzinger S, Mertsch S, Grässel S, Paulus W. Collagen XVI expression is upregulated in glioblastomas and promotes tumor cell adhesion. *FEBS Lett*. 2008;582(23–24):3293–300. <https://doi.org/10.1016/j.febslet.2008.09.017>. (Epub 2008 Sep 17 PMID: 18804107).
 47. Mao P, Wang T, Du CW, Yu X, Wang MD. CXCL5 promotes tumorigenesis and angiogenesis of glioblastoma via JAK-STAT/NF- κ b signaling pathways. *Mol Biol Rep*. 2023;50(10):8015–23. <https://doi.org/10.1007/s11033-023-08671-3>. (Epub 2023 Aug 4 PMID: 37541997).
 48. Filippova N, Grimes JM, Leavenworth JW, Namkoong D, Yang X, King PH, Crowley M, Crossman DK, Nabors LB. Targeting the TREM1-positive myeloid microenvironment in glioblastoma. *Neurooncol Adv*. 2022 Sep 15;4(1):vdac149. <https://doi.org/10.1093/oaajnl/vdac149>. Erratum in: *Neurooncol Adv*. 2023 Jan 05;5(1):vdac189. PMID: 36249290; PMCID: PMC9555298.
 49. Ajith A, Mamouni K, Horuzsko DD, Musa A, Dzutsev AK, Fang JR, Chadli A, Zhu X, Lebedyeva I, Trinchieri G, Horuzsko A. Targeting TREM1 augments antitumor T cell immunity by inhibiting myeloid-derived suppressor cells and restraining anti-PD-1 resistance. *J Clin Invest*. 2023;133(21):e167951. <https://doi.org/10.1172/JCI167951>. PMID:37651197;PMCID:PMC10617775.

Publisher's Note

Springer Nature remains neutral with regard to jurisdictional claims in published maps and institutional affiliations.